Undulator Radiation and its Application to Beam Diagnostics

(1) Accelerator diagnostics beamline II (BL05SS)

BL05SS has an insertion device light source, two optics hutches, and an experiment hutch. The insertion device (ID05) is of out-vacuum type and designed to be able to fit many kinds of experiments. The mounted pure-permanent magnet array, which is made of the ternary alloy Ne-Fe-B (NEOMAX-44H), is of planar Halbach type with the 51 periods of 76 mm long. When the magnet gap is a minimum value of 20 mm generating a peak field of 0.82 T, the deflection parameter K is a maximum value of 5.8, which leads to a multi-pole wiggler (MPW) radiation produced on the many higher-order harmonics that are useful for electron beam diagnostics. The MPW can emit the total radiation power of 10.4 kW when the electron beam current is 100 mA. By widening the magnet gap, ID05 as an undulator with small K can be also useful for the experiments requiring the higher spectral photon flux and the lower heat load to avoid the thermal drift of a frontend slit or the monochromator.

The layout of the X-ray transport channel of BL05SS is shown in Fig.1. The front end has a X-slit and a Y-slit to shape the white X-ray beam of the ID05. The optics hutch I has the graphite filters and the metal (aluminum) filters, which have moving mechanisms to adjust the intensities and the spectrum of white X-ray beam. The optics hutch II has a cryogenic double crystal monochromator, which covers the photon energy range of 4 to 38 keV by (111) reflection of silicon crystals. Beryllium windows installed in the experimental hutch allow us to handle the monochromatic X-ray beam in atmosphere. To develop techniques for the beam diagnostics based on observations of synchrotron radiations (SR), in the experimental hatch, we can measure energy spectra, angular spectral fluxes and temporal structures of undulator radiations from ID05.

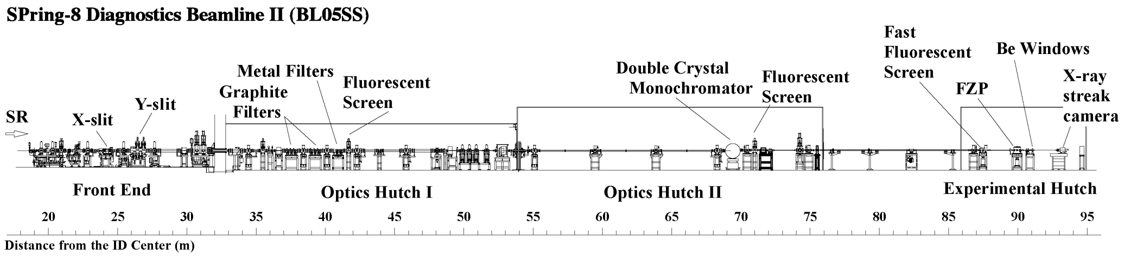

Figure 1: Schematic view of the SPring-8 diagnostics beamline II (BL05SS).

(2) Energy spectrum & Angular spectral flux of ID radiation

The energy spectrum produced by a filament electron beam in a given direction consists of a series of harmonic peaks, the frequency of which are multiples of the fundamental resonant frequency ω_1. For a planar undulator, ω_1 is given by

$$\omega_1 = \frac{2c\gamma^2}{\lambda_u\left(1 + K^2/2 + \gamma^2\theta_x^2 + \gamma^2\theta_y^2\right)} \quad , \qquad \text{eq. (1)}$$

where λ_u, K, γ, c, and (θ_x, θ_y) are the period length, the deflection parameter, the electron beam energy divided by mc^2, the light speed, and the angle between the electron and the observer, respectively. For a single electron and an observation point, the lobe of on-axis emission is zero for all even harmonics 2, 4, 6, while it reaches a maximum for the odd harmonics 1, 3, 5, the spectrum widths of which are equal to $1/nN$ where n is the harmonic number and N is the number of periods. For a given point of observation, all electrons of a thick beam do not have the same resonant frequency ω_1. This can occur through the angular divergence of the electron beam, which spreads both the horizontal and vertical angles of (θ_x, θ_y). A spread of the transverse position of the electron beam also induces a spread of ω_1 because an observer located sufficiently close to the source point sees the radiation emitted by the various electrons under a different angle (θ_x, θ_y). Equation (1) indicates that the spread in the angle θ_x and θ_y shifts the resonant frequency ω_1 to the lower energy side only. As a result, the electron beam emittance leads to the low energy tail of the spectrum through a slit. The energy spread of electron beam also has an effect on a spread of ω_1. If the relative energy spread σ/γ of the electron beam is

Gaussian, it introduces a Gaussian spread in the spectrum of each harmonic:

$$\frac{\sigma_\omega}{\omega} = 2\frac{\sigma_\gamma}{\gamma} \quad . \qquad \text{eq. (2)}$$

To be summarized as follows, the peak of the harmonics observed on-axis of the electron beam always has a steep slope on the high energy side which is dominated by nN and by σ_γ/γ, and has a reduced slope on the low energy side which is dominated by the emittance, beta function and observation aperture limited by the finite slit width.

The energy spectrum is obtained by measuring the spectral photon flux using an ionization chamber set up in atmosphere, while changing the energy of monochromatic X-ray by scanning Bragg angle of the Si(111) double-crystal monochromator. A rectangular tantalum slit is placed in front of the ionization chamber to measure the on-axis photon flux of ID05. The aperture of the slit was 4.2 μrad × 4.2 μrad. The nominal equilibrium emittance and relative energy spread of 8 GeV stored electron beam are 3.4 nm.rad and 1.1×10^{-3}, respectively. A typical example of the energy spectrum of the fundamental harmonic measured at the magnet gap of 80 mm, which gives the deflection parameter K of 0.45, is shown in Fig.2. The tail of the low energy side comes from the horizontal emittance. The effect of the slit aperture is negligibly small. The slope on the high-energy side is dominated by $1/nN$~0.02. The energy spread has a negligible effect on it. When the magnet gap is the minimum value of 20 mm, the deflection parameter K of 5.8 leads to the fundamental harmonic of 0.45 keV. As a consequence, many higher-order harmonics are observed in the photon energy range of 4 to 30 keV (Fig. 3). For the harmonics higher than the 19th, the energy spread has the non-negligible effect on the slope of the high-energy side.

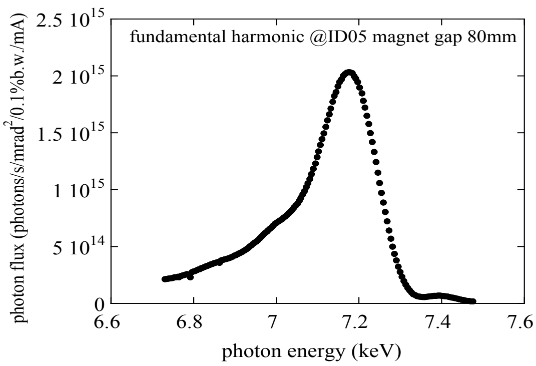

Figure 2: Measured on-axis energy spectrum of the fundamental harmonic when the magnet gap is 80 mm. The deflection parameter K is 0.45.

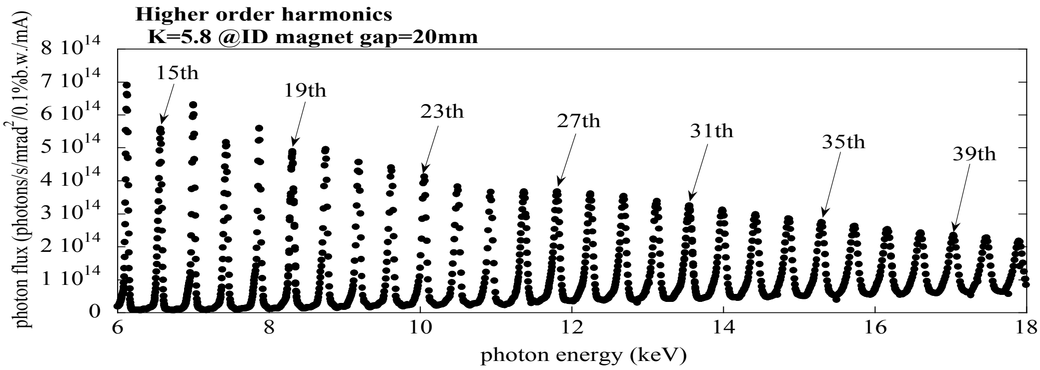

Figure 3: On-axis energy spectrum measured at the minimum magnet gap of 20 mm, which gives the deflection parameter K of 5.8. We can see many higher-order harmonics.

Angular spectral photon flux can be also observed using an X-ray CCD camera. Fig. 4 shows an example of the angular spectral flux observed at the photon energy of 8.3 keV, which corresponds to the peak of the 19th harmonic for the magnet gap of 20 mm. The center spot is the spatial profile of the 19th harmonic. The outer rings correspond to the off-axis radiations of the 20th and 21st harmonics. The horizontal width of the center spot is determined by the horizontal angular divergence of electron beam, while the vertical width is dominated by the energy spread of electron beam and the intrinsic angular divergence $(\lambda/2L)^{1/2}$ of undulator radiation, where λ and L are the wavelength of the radiation and the total length of ID, respectively. The vertical angular divergence of electron beam has a negligible effect due to small emittance coupling ratio.

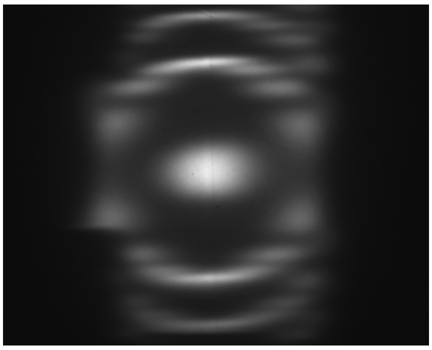

Figure 4: Observed angular spectral flux at the photon energy of 8.3 keV corresponding to the peak of the 19th harmonic for the minimum magnet gap of 20 mm. The center spot is the 19th harmonic radiation, and two outer rings correspond to the off-axis radiations of the 20th and 21st harmonics.

(3) Observation of stored beam oscillation at the injection timing by using a Turn-by-Turn Beam Profile Monitor (TTPM)

At the diagnostics beamline II with the ID light source, the turn-by-turn beam profile monitor (TTPM) [1] observing monochromatic photon beam profiles of the ID has been developed. It enables us to observe fast phenomena such as oscillations of the stored beam at injections for topping-up, blowups of transverse size and energy spread of a high-current single bunch caused by beam instabilities, and so on. The experimental setup of the TTPM is shown in Fig. 5. It consists of a YAG (Ce) screen with decay time of several tens of nano seconds, imaging optics and a fast CCD camera with an image intensifier (I.I.). The imaging optics of the TTPM transforms the 2D beam profile on the YAG (Ce) screen to the two line profiles projected on the horizontal and the vertical axes, respectively. The fast gate by the micro channel plates (MCPs) of the I.I. selects the light from specific bunches out of the whole stored bunches. The kinetics readout mode of the fast CCD camera (Roper Scientific: ProEM 512B) enables measurements with high repetition rates. In Fig. 6 we show an example of angular oscillation of the photon beam axis of the ID observed with the TTPM at the topping-up beam injection in the user time. For injection, four bump magnets are excited by four individual pulsed power supplies to generate a pulsed bump orbit. A residual kick caused by the non-similarity of the temporal shape of the magnetic fields of the four pulsed magnets could excite a horizontal oscillation of the stored beam. Efforts have been made by tuning the fields of the four bump magnets to reduce the residual kick and by applying a counter kick of a fast correction magnet to the residual kick [2,3]. While the residual kick at the temporal peak of the bump magnetic fields has been succesfully suppressed, there still remains a significant kick to the stored beam at the rising part of the fields. Figure 2 shows the profiles of the photon beam of the ID obtained every 5 turns by using the kinetics readout mode of the fast CCD camera, by selecting with the I.I. those bunches suffered residual kick at the rising part of the bump magnetic fields. The maximum oscillation amplitude just after the injection turn corresponds to the angle of 20 μrad, which will hopefully be reduced by further tuning of the fast correction magnet based on the oscillation measurements by the TTPM.

[1] M. Masaki et al., "Development of Turn-by-Turn Diagnostic System Using Undulator Radiation", Proceedings of IBIC2012, Tsukuba, Japan, http://ibic12.kek.jp/prepress/papers/tupb63.pdf
[2] SPring-8 Research Frontiers 2009, p.154.
[3] SPring-8 Research Frontiers 2010, p.152

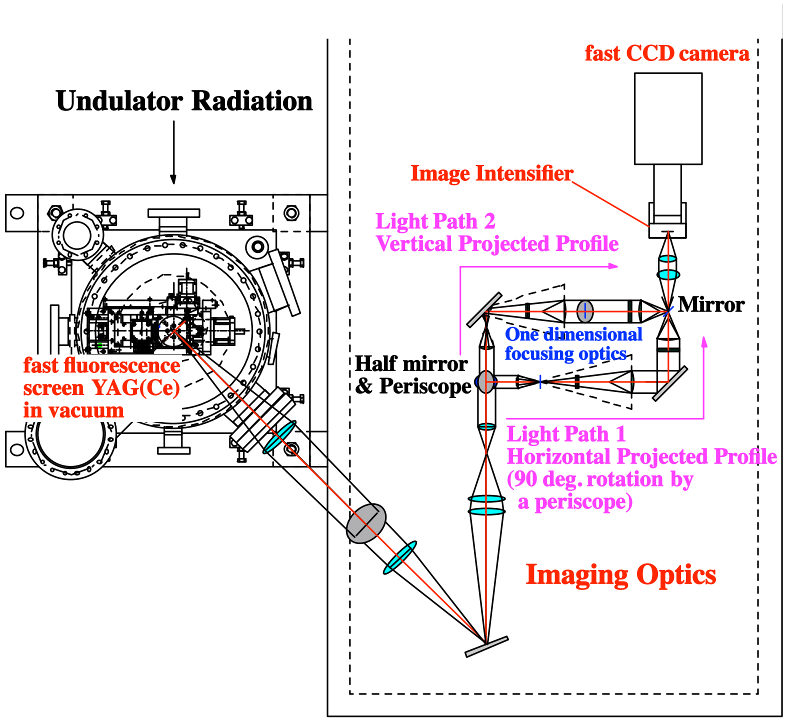

Figure 5: Experimental setup of the turn-by-turn beam profile monitor (TTPM) developed at the diagnostics beamline II (BL05SS).

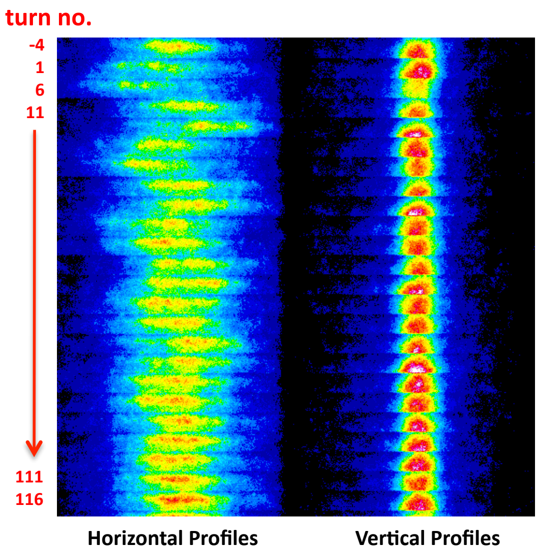

Figure 6: An example of the profiles of the photon beam of the ID obtained every 5 turns by the TTPM. The left and right images are for horizontal and vertical profiles, respectively. The numbers on the left side show the turn numbers after injection for topping-up of which the turn of the bump orbit excitation is labeled as the zeroth turn (see text).